Applied Physics Letters

Epitaxial stabilization of ultra thin films of high entropy perovskite

Cite as: Appl. Phys. Lett. **116**, 071601 (2020); https://doi.org/10.1063/1.5133710
Submitted: 25 October 2019 • Accepted: 30 January 2020 • Published Online: 18 February 2020

Ranjan Kumar Patel, Shashank Kumar Ojha, Siddharth Kumar, et al.

Applied Physics Letters ARTICLE scitation.org/journal/apl

Epitaxial stabilization of ultra thin films of high entropy perovskite

Cite as: Appl. Phys. Lett. **116**, 071601 (2020); doi: 10.1063/1.5133710
Submitted: 25 October 2019 · Accepted: 30 January 2020 ·
Published Online: 18 February 2020

View Online Export Citation CrossMark

Ranjan Kumar Patel,[1] Shashank Kumar Ojha,[1] Siddharth Kumar,[1] Akash Saha,[2] Prithwijit Mandal,[1] J. W. Freeland,[3] and S. Middey[1,a)]

AFFILIATIONS

[1]Department of Physics, Indian Institute of Science, Bengaluru 560012, India
[2]Undergraduate Programme, Indian Institute of Science, Bengaluru 560012, India
[3]Advanced Photon Source, Argonne National Laboratory, Argonne, Illinois 60439, USA

[a)]Electronic mail: smiddey@iisc.ac.in

ABSTRACT

High entropy oxides (HEOs) are a class of materials, containing equimolar portions of five or more transition metal and/or rare-earth elements. We report here about the layer-by-layer growth of HEO [$(La_{0.2}Pr_{0.2}Nd_{0.2}Sm_{0.2}Eu_{0.2})NiO_3$] thin films on $NdGaO_3$ substrates by pulsed laser deposition. The combined characterizations with *in situ* reflection high energy electron diffraction, atomic force microscopy, and x-ray diffraction affirm the single crystalline nature of the film with smooth surface morphology. The desired +3 oxidation of Ni has been confirmed by an element sensitive x-ray absorption spectroscopy measurement. Temperature dependent electrical transport measurements revealed a first order metal-insulator transition with the transition temperature very similar to the undoped $NdNiO_3$. Since both these systems have a comparable tolerance factor, this work demonstrates that the electronic behaviors of *A*-site disordered perovskite-HEOs are primarily controlled by the average tolerance factor.

Finding ways to tune materials' properties is essential for fulfilling the demand of the constantly evolving modern technology. Transition metal oxides show various fascinating electronic and magnetic phenomena such as metal-insulator transition, superconductivity, colossal magnetoresistance, multiferroicity, skyrmions, etc., which have a lot of prospect for technological applications.[1–6] Furthermore, transition metal (TM) based high entropy oxides (HEOs) have been explored in recent years to achieve tunable properties in unexplored parts of the complex phase diagram.[7–21] In general, the configurational entropy of a multicomponent solid solution can be enhanced by mixing a large number of cations in equiatomic proportions and a single structural phase is formed if the entropy contribution overcomes enthalpy driven phase separation ($\Delta G_{mix} = \Delta H_{mix} - T\Delta S_{mix}$; ΔG_{mix}, ΔH_{mix}, ΔS_{mix} are the Gibbs free energy, enthalpy, and entropy of mixing, respectively).[7,18] After the report of the first HEO ($Mg_{0.2}Ni_{0.2}Co_{0.2}Cu_{0.2}Zn_{0.2}O$ with a rock salt structure) by Rost *et al.*,[7] HEOs with other structural symmetry such as perovskite[15,17] and spinel[16] have also been synthesized. However, this promising field of HEO is at a very early stage and most of the aspects of HEOs are yet to be explored experimentally. For example, it is still unknown whether the strong disorder or the average tolerance factor (t_{avg}) determines the electronic and magnetic behaviors of perovskite HEOs.

As a prototypical example of perovskite (ABO_3) series, $RENiO_3$ (RE= La, Pr, Nd, Sm, Eu…Lu) exhibits an interesting phase diagram as a function of tolerance factor ($t=\frac{R_{RE}+R_O}{\sqrt{2}(R_{Ni}+R_O)}$, where R_{RE}, R_{Ni}, R_O are the ionic radii of RE, Ni, and O, respectively).[22,23] $LaNiO_3$, the least distorted member of this series, remains metallic and paramagnetic down to the lowest temperature. Bulk $PrNiO_3$ and $NdNiO_3$ (NNO) show temperature driven simultaneous transitions from an orthorhombic, paramagnetic, and metallic phase to a monoclinic, antiferromagnetic, and insulating phase, respectively [see Fig. 1(a)]. The insulating phase is also characterized by a checkerboard type charge ordering.[24] In the case of more distorted members, such as $SmNiO_3$, $EuNiO_3$, etc., the magnetic transition gets decoupled from the other three simultaneous transitions, resulting in an intermediate paramagnetic, insulating, and charge ordered phase. The quest to understand the origin of these transitions has led to remarkable progress in epitaxial stabilization of the $RENiO_3$ family (see Refs. 25 and 26 and literature cited therein), and thin films of $RENiO_3$ with RE = La, Pr, Nd, Sm, and Eu have been stabilized so far.[25–37] This further provides a

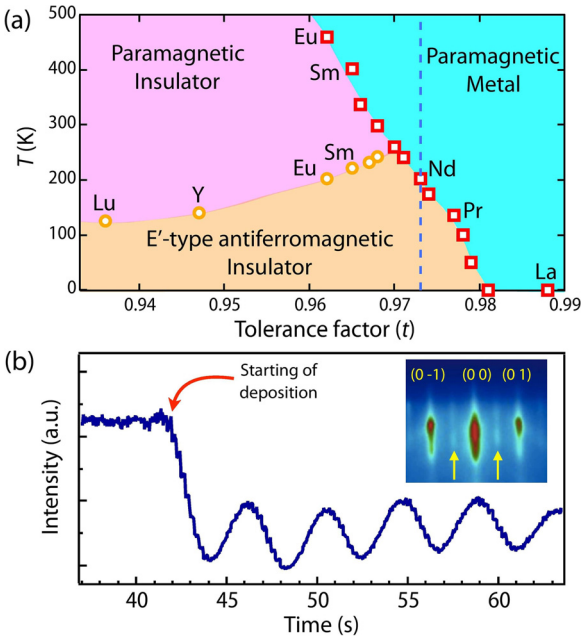

FIG. 1. (a) Phase diagram of $RENiO_3$ series, following Ref. 40. Reproduced with permission from Zhou *et al.*, Phys. Rev. B **67**, 020404 (2003). Copyright 2003 American Physical Society. The dotted line represents the average of the tolerance factors of $LaNiO_3$, $PrNiO_3$, $NdNiO_3$, $SmNiO_3$, and $EuNiO_3$. (b) Temporal variations of specular spot intensity of the RHEED pattern during the growth of the (LPNSE)NO film on the NGO substrate. The RHEED image of the film after cooling is shown in the inset.

unique opportunity to verify the role of disorder vs t_{avg} in determining the electronic and magnetic properties of perovskite HEO with a strong disorder at the *A* site.

In this Letter, we report layer-by-layer growth of $(La_{0.2}Pr_{0.2}Nd_{0.2}Sm_{0.2}Eu_{0.2})NiO_3$ [(LPNSE)NO] thin films on a single crystalline $NdGaO_3$ (NGO) substrate by pulsed laser deposition (PLD). The variation in bulk lattice constants together with the pseudo-cubic lattice constants of several members of the $RENiO_3$ series is shown in Table I. Since the average of *t* of $RENiO_3$ with *RE* = La, Pr, Nd, Sm, Eu [indicated by a vertical line in Fig. 1(a)] is comparable to NNO, the electronic behavior of [(LPNSE)NO] thin films has also been compared with that of NNO films. Several characterization techniques including *in situ* RHEED (reflection high energy electron diffraction) and ex-situ atomic force microscopy (AFM), x-ray diffraction (XRD), and x-ray absorption spectroscopy (XAS) confirmed high structural quality of these (LPNSE)NO] thin films with a proper oxidation state of Ni. Transport measurements and XAS experiments further revealed that in-spite of having a strong structural disorder, the electronic behaviors of the (LPNSE)NO sample are very similar to a single *A* site cation NNO film.

TABLE I. Lattice parameters (*a*, *b*, and *c*) of few rare earth nickelates. Pseudo cubic lattice constants a_{pc}, b_{pc}, and c_{pc} are also listed. For orthorhombic systems, $a_{pc} = b_{pc} = \sqrt{a^2 + b^2}/2$ and $c_{pc} = c/2$.

Compound	*a* (Å)	*b* (Å)	*c* (Å)	$a_{pc} = b_{pc}$ (Å)	c_{pc} (Å)	References
$LaNiO_3$	5.457	5.457	13.146	3.838	3.838	38
$PrNiO_3$	5.419	5.380	7.626	3.818	3.813	38
$NdNiO_3$	5.389	5.382	7.610	3.808	3.805	38
$SmNiO_3$	5.327	5.432	7.565	3.804	3.782	39
$EuNiO_3$	5.294	5.458	7.537	3.802	3.769	39

(LPNSE)NO films with thicknesses of 15 uc, 30 uc, and 45 uc (uc = unit cell in pseudocubic notation) and the NNO film with a thickness of 15 uc were grown on NGO $(110)_{or}$ $[(001)_{pc}]$ substrates (here, or and pc denote the orthorhombic and pseudocubic setting) by a PLD system at 735 °C under a dynamic oxygen pressure of 100–150 millitorr. The details of the target preparation can be found in the supplementary material. A KrF excimer laser, operating with 4 Hz and an energy density of 1.5 J/cm^2, was used for the deposition. The layer by layer growth was monitored by using a high pressure RHEED system. The films were post-annealed at the growth temperature under an oxygen pressure of 500 Torr for 30 min and cooled to room temperature at the same oxygen pressure. A Park system AFM was used to check the morphology of these films. X-ray diffraction patterns were recorded using a Rigaku Smartlab x-ray diffractometer. Temperature dependent resistivity was measured by using the Van der Pauw geometry in a Quantum Design PPMS (physical property measurement system). XAS spectra at Ni-$L_{3,2}$ and O-*K* edges were collected in bulk-sensitive (probing depth ~20 nm) TFY (total fluorescence yield) mode at the 4-ID-C beamline of the Advanced Photon Source, Argonne National Laboratory.

The time dependent intensity of the specular reflection of the RHEED pattern [Fig. 1(b)], recorded during the deposition, shows very prominent oscillations, confirming the layer-by-layer growth of the (LPNSE)NO film. The inset of Fig. 1(b) shows a RHEED image of a (LPNSE)NO film, taken after cooling to room temperature. The streaky pattern of specular (0 0) and off-specular (0 1), (0–1) Bragg reflections is a characteristic of smooth surface morphology. Akin to the RHEED pattern of the NNO film on the NGO substrate,[41] (LPNSE)NO films also have half-order spots: (0 1/2) and (0 −1/2) (denoted by the arrows), indicating orthorhombic/monoclinic symmetry at room temperature.[42] The inset of Fig. 2(a) shows the AFM image of the 45 uc (LPNSE)NO film, and the roughness is found to be ~1.8 Å well below c_{pc}, further testifying excellent surface morphology of the film.

In order to check the structural quality of the samples and to detect the presence of any impurity phase, we have recorded 2θ-ω diffraction scan for (LPNSE)NO films using Cu K_α radiation. Such a long scan XRD for the 45 uc (LPNSE)NO film [Fig. 2(a)] consists of broad film peaks in the vicinity of sharp substrate peaks, confirming the single crystalline nature of the film. Most importantly, the absence of any impurity peaks (within the detection limit of XRD) infers the growth conditions used in this work is able to stabilize the multicomponent system into a single phase. XRD patterns around the $(0\,0\,2)_{pc}$ substrate peak for 15 uc, 30 uc, and 45 uc (LPNSE)NO films are shown in Figs. 2(b)–2(d), respectively. The very close proximity between the film peak and the substrate peak [Fig. 2(b)] in the case of the 15 uc (LPNSE)NO film prohibits a reliable estimation of the out-of-plane lattice constant (c_{pc}). c_{pc} values for 30 uc and 45 uc films are found to be 3.792 Å and 3.784 Å, respectively. The presence of thickness fringes in the vicinity of the film peaks further supports the excellent flatness

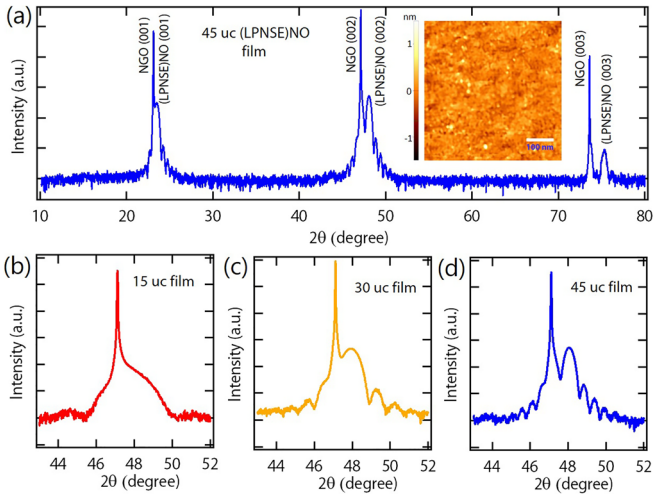

FIG. 2. (a) Long 2θ-ω XRD scan for the 45 uc (LPNSE)NO film. (b)-(d) XRD patterns of 15, 30, and 45 uc films near the NGO (002)pc peak, respectively. AFM surface morphology of the 45 uc film is shown in the inset of (a).

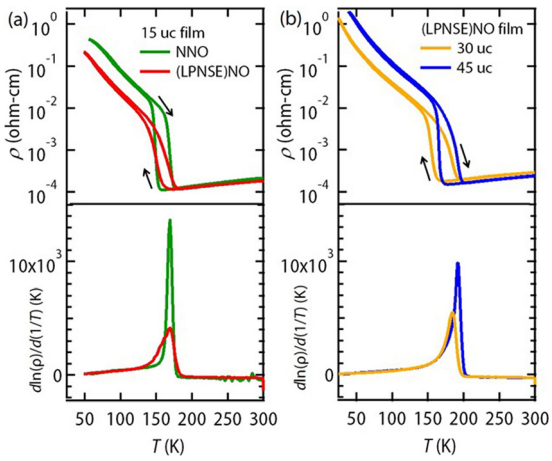

FIG. 3. Temperature dependent resistivities of 15 uc NNO and 15 uc (LPNSE)NO films [30 uc and 45 uc (LPNSE)NO film] are shown in the upper panel of (a) [(b)]. Estimation of T_N from $d\ln(\rho)/d(1/T)$ vs T analysis (heating run) is plotted in the corresponding lower panel.

of the film-substrate interface. Rocking curve XRD further supports extremely high quality of the film, and ϕ scan XRD establishes the same in-plane orientation of the (LPNSE)NO film and NGO substrate (see the supplementary material). The thickness of the films calculated from the position of the fringes (e.g., ∼17.3 nm for 45 uc film) are close to the value expected from the RHEED oscillations. The c_{pc} value of the 15 uc NNO film is found to be 3.845 Å (XRD pattern not shown). Complimentary experiments like synchrotron based x-ray diffraction and extended x-ray absorption fine structure (EXAFS) experiments will be required to understand the difference in c_{pc} between (LPNSE)NO and NNO films.

After confirming the high structural and morphological quality, we have investigated the electrical transport of the films. As reported earlier,[28,31,41] the 15 uc NNO thin film on the NGO substrate undergoes first order MIT [upper panel of Fig. 3(a)]. The transition temperature in the cooling run ($T^c_{MIT} \sim 160$ K) and in the heating run ($T^h_{MIT} \sim 180$ K) is lower compared to the bulk NNO and is related to the epitaxial strain and finite thickness.[28] Surprisingly, the resistivity (ρ) of the 15 uc (LPNSE)NO film at 300 K is very similar to that of the 15 uc NNO film in-spite of having a strong disorder on the A site. It further exhibits a MIT with strong thermal hysteresis ($T^c_{MIT} \sim 175$ K, $T^h_{MIT} \sim 185$ K). However, the transition is more sluggish and ρ of the insulating phase is also lower than that of the 15 uc NNO film. With the increase in the film thickness, T_{MIT} becomes approximately 200 K [upper panel of Fig. 3(b)], which is very close to the transition temperature expected for the corresponding t of the (LPNSE)NO phase from the bulk phase diagram [Fig. 1(a)]. This finding clearly establishes that the average tolerance factor controls T_{MIT} for this HEO, rather than the disorder at the A-site.

All RENiO$_3$ with an insulating phase also hosts E'-type antiferromagnetic ordering.[28,32,42–45] The magnetic transition temperature (T_N) can be approximately estimated from the $d(\ln\rho)/d(1/T)$ vs T plot, as demonstrated recently for NNO films and EuNiO$_3$/LaNiO$_3$ superlattices.[41,45,46] Such resistivity analysis of the heating run data [lower panel of Figs. 3(a) and 3(b)] provides a T_N value of 170 K for both 15 uc NNO and 15 uc (LPNSE)NO samples, 185 and 190 K for 30 uc and 45 uc (LPNSE)NO films, respectively. This suggests simultaneous electronic and magnetic transitions in these (LPNSE)NO films. Soft x-ray resonant scattering experiments can further confirm this.[28,32,42,44,45]

The required high +3 oxidation state of Ni makes RENiO$_3$ based systems very susceptible to oxygen nonstoichiometry. In order to further understand the electronic and chemical structures of these films, we have measured XAS spectra on the Ni $L_{3,2}$ edge and O-K edge at 300 K and 85 K (much below T_{MIT}). Due to the strong overlap of the La M_4 edge with Ni L_3 for the (LPNSE)NO film, we discuss here only the L_2 edge. First of all, the XAS line shape of both 15 uc NNO and 15 uc (LPNSE)NO films at 300 K [Fig. 4(a)] is consistent with Ni^{3+} in the metallic phase of nickelates,[49–52] affirming the stabilization of the desired oxidation state of Ni. Further, the appearance of strong multiple structures (around 870.05 eV) in the insulating phase of the (LPNSE)NO film is also consistent with the observation of the NNO film [Fig. 4(a)] and the insulating phase of other nickelates.[30,49–51] Similar to the high T_c cuprates, RENiO$_3$ also contains ligand holes, which can be observed as a pre-peak around 528 eV in the O-K edge XAS spectrum due to the $d^8\underline{L} \rightarrow \underline{c}d^8$ ($\underline{c}$ denotes the hole in the oxygen 1s core state and $\underline{L}$ corresponds to a hole in the O 2p state).[28,46,49,52,53] While the intensity of the pre peak is reduced in the (LPNSE)NO film at 300 K, the position and FWHM (full width at half maxima) are very similar for both samples. The measurements at 85 K have found lowering of the peak width in both samples (not shown), which is expected due to the band narrowing across the MIT.[53,54] Thus, transport and XAS measurements conclude that the overall electronic structure effect across the MIT of the (LPNSE)NO film is very similar to that of the NNO film.

To summarize, we have grown high quality epitaxial films of multicomponent (LPNSE)NO in a layer-by-layer fashion by pulsed laser deposition. RHEED, XRD, AFM, XAS, and transport measurements have been carried out to investigate the structure and the electronic behavior of these films. In spite of having multi elements and strong disorder at the RE site, the average tolerance factor determines

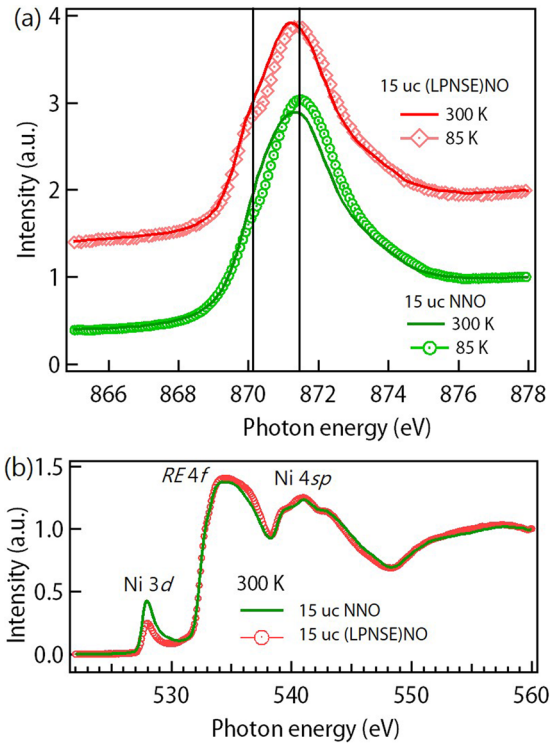

FIG. 4. (a) Ni L_2-edge and (b) O-*K* edge XAS for 15 uc NNO and 15 uc (LPNSE)NO films on the NGO substrate. Ni L_2 edge data has been moved vertically for visual clarity. In the O-*K* edge XAS spectra, the pre-peak around 528 eV is related to the transition from O 1*s* to the Ni 3*d* -O 2*p* hybridized states. The lower intensity of this pre-peak for the (LPNSE)NO film compared to NNO is likely to be related to the structural disorder.[47,48] 4*f* and 5*d* hybridized states of rare earth (*RE*) ions, present in the sample and substrate, result in the peak around 534–535 eV. Ni 4*s* and 4*p* also hybridized with O 2*p*, resulting in the peaks around 540–545 eV.

the electronic transition temperature. However, the microscopic details, e.g., nucleation of the insulating/metallic phase around the transition temperature,[55] charge transfer between Ni and *RE* sites,[56] conductivity noise,[57] etc., may depend on the details of the *RE* composition and need to be explored further. Stabilization of such a multi *RE* system in a single crystalline form would further allow us to investigate the complexity of phase transitions around the triple point of the $RENiO_3$ phase diagram.[58] Due to the chemical diversity of the perovskite family, huge numbers of HEO with a strong disorder at the *A* site or the *B* site or both the sites can be studied in the future to explore disorder driven physics in strongly correlated systems.

See the supplementary material for the details of target preparation, results of the rocking curve, and phi scan in XRD.

This work was funded by a DST Nanomission Grant (No. DST/NM/NS/2018/246) and a SERB Early Career Research Award (No. ECR/2018/001512). The authors acknowledge AFM and XRD facilities at the Department of Physics, IISc Bangalore. RKP and SM thank the Department of Science and Technology, India (No. SR/NM/Z-07/2015) for the financial support to conduct the synchrotron experiment at the Advanced Photon Source and Jawaharlal Nehru Centre for Advanced Scientific Research (JNCASR) for managing the project. This research used resources of the Advanced Photon Source, a U.S. Department of Energy Office of Science User Facility operated by the Argonne National Laboratory under Contract No. DE-AC02-06CH11357.

REFERENCES

[1]M. Imada, A. Fujimori, and Y. Tokura, Rev. Mod. Phys. **70**, 1039 (1998).
[2]Y. Tokura, Rep. Prog. Phys. **69**, 797 (2006).
[3]Z. Yang, C. Ko, and S. Ramanathan, Annu. Rev. Mater. Res. **41**, 337 (2011).
[4]G. Catalan, J. Seidel, R. Ramesh, and J. F. Scott, Rev. Mod. Phys. **84**, 119 (2012).
[5]M. Lorenz, M. R. Rao, T. Venkatesan, E. Fortunato, P. Barquinha, R. Branquinho, D. Salgueiro, R. Martins, E. Carlos, A. Liu *et al.*, J. Phys. D: Appl. Phys. **49**, 433001 (2016).
[6]J. Matsuno, J. Fujioka, T. Okuda, K. Ueno, T. Mizokawa, and T. Katsufuji, Sci. Technol. Adv. Mater. **19**, 899 (2018).
[7]C. M. Rost, E. Sachet, T. Borman, A. Moballegh, E. C. Dickey, D. Hou, J. L. Jones, S. Curtarolo, and J.-P. Maria, Nat. Commun. **6**, 8485 (2015).
[8]D. Bérardan, S. Franger, A. Meena, and N. Dragoe, J. Mater. Chem. A **4**, 9536 (2016).
[9]C. M. Rost, Z. Rak, D. W. Brenner, and J.-P. Maria, J. Am. Ceram. Soc. **100**, 2732 (2017).
[10]A. Sarkar, R. Djenadic, N. J. Usharani, K. P. Sanghvi, V. S. Chakravadhanula, A. S. Gandhi, H. Hahn, and S. S. Bhattacharya, J. Eur. Ceram. Soc. **37**, 747 (2017).
[11]R. Djenadic, A. Sarkar, O. Clemens, C. Loho, M. Botros, V. S. Chakravadhanula, C. Kübel, S. S. Bhattacharya, A. S. Gandhi, and H. Hahn, Mater. Res. Lett. **5**, 102 (2017).
[12]S. Jiang, T. Hu, J. Gild, N. Zhou, J. Nie, M. Qin, T. Harrington, K. Vecchio, and J. Luo, Scr. Mater. **142**, 116 (2018).
[13]G. Anand, A. P. Wynn, C. M. Handley, and C. L. Freeman, Acta Mater. **146**, 119 (2018).
[14]A. Sarkar, L. Velasco, D. Wang, Q. Wang, G. Talasila, L. de Biasi, C. Kübel, T. Brezesinski, S. S. Bhattacharya, H. Hahn *et al.*, Nat. Commun. **9**, 3400 (2018).
[15]Y. Sharma, B. L. Musico, X. Gao, C. Hua, A. F. May, A. Herklotz, A. Rastogi, D. Mandrus, J. Yan, H. N. Lee *et al.*, Phys. Rev. Mater. **2**, 060404 (2018).
[16]J. Dkabrowa, M. Stygar, A. Mikua, A. Knapik, K. Mroczka, W. Tejchman, M. Danielewski, and M. Martin, Mater. Lett. **216**, 32 (2018).
[17]R. Witte, A. Sarkar, R. Kruk, B. Eggert, R. A. Brand, H. Wende, and H. Hahn, Phys. Rev. Mater. **3**, 034406 (2019).
[18]A. Sarkar, Q. Wang, A. Schiele, M. R. Chellali, S. S. Bhattacharya, D. Wang, T. Brezesinski, H. Hahn, L. Velasco, and B. Breitung, Adv. Mater. **31**, 1806236 (2019).
[19]J. Zhang, J. Yan, S. Calder, Q. Zheng, M. A. McGuire, D. L. Abernathy, Y. Ren, S. H. Lapidus, K. Page, H. Zheng *et al.*, Chem. Mater. **31**, 3705–3711 (2019).
[20]P. Meisenheimer, T. Kratofil, and J. Heron, Sci. Rep. **7**, 13344 (2017).
[21]Y. Sharma, Q. Zheng, A. R. Mazza, E. Skoropata, T. Heitmann, Z. Gai, B. Musico, P. F. Miceli, B. C. Sales, V. Keppens *et al.*, preprint arXiv:1909.05019 (2019).
[22]M. L. Medarde, J. Phys.: Condens. Matter **9**, 1679 (1997).
[23]G. Catalan, Phase Trans. **81**, 729 (2008).
[24]U. Staub, G. I. Meijer, F. Fauth, R. Allenspach, J. G. Bednorz, J. Karpinski, S. M. Kazakov, L. Paolasini, and F. d'Acapito, Phys. Rev. Lett. **88**, 126402 (2002).
[25]S. Middey, J. Chakhalian, P. Mahadevan, J. W. Freeland, A. J. Millis, and D. D. Sarma, Annu. Rev. Mater. Res. **46**, 305 (2016).
[26]S. Catalano, M. Gibert, J. Fowlie, J. Íñiguez, J.-M. Triscone, and J. Kreisel, Rep. Prog. Phys. **81**, 046501 (2018).
[27]S. D. Ha, M. Otaki, R. Jaramillo, A. Podpirka, and S. Ramanathan, J. Solid State Chem. **190**, 233 (2012).
[28]J. Liu, M. Kargarian, M. Kareev, B. Gray, P. J. Ryan, A. Cruz, N. Tahir, Y.-D. Chuang, J. Guo, J. M. Rondinelli, J. W. Freeland, G. A. Fiete, and J. Chakhalian, Nat. Commun. **4**, 2714 (2013).
[29]L. Feigl, B. Schultz, S. Ohya, D. Ouellette, A. Kozhanov, and C. Palmstram, J. Cryst. Growth **366**, 51 (2013).

[30]D. Meyers, S. Middey, M. Kareev, M. van Veenendaal, E. J. Moon, B. A. Gray, J. Liu, J. W. Freeland, and J. Chakhalian, Phys. Rev. B **88**, 075116 (2013).
[31]E. Mikheev, A. J. Hauser, B. Himmetoglu, N. E. Moreno, A. Janotti, C. G. Van de Walle, and S. Stemmer, Sci. Adv. **1**, e1500797 (2015).
[32]M. Hepting, M. Minola, A. Frano, G. Cristiani, G. Logvenov, E. Schierle, M. Wu, M. Bluschke, E. Weschke, H.-U. Habermeier, E. Benckiser, M. L. Tacon, and B. Keimer, Phys. Rev. Lett. **113**, 227206 (2014).
[33]R. Scherwitzl, S. Gariglio, M. Gabay, P. Zubko, M. Gibert, and J.-M. Triscone, Phys. Rev. Lett. **106**, 246403 (2011).
[34]F. Y. Bruno, K. Z. Rushchanskii, S. Valencia, Y. Dumont, C. Carrétéro, E. Jacquet, R. Abrudan, S. Blügel, M. Ležaić, M. Bibes, and A. Barthélémy, Phys. Rev. B **88**, 195108 (2013).
[35]P. King, H. Wei, Y. F. Nie, M. Uchida, C. Adamo, S. Zhu, X. He, I. Božović, D. G. Schlom, and K. M. Shen, Nat. Nanotechnol. **9**, 443 (2014).
[36]A. S. Disa, D. Kumah, J. Ngai, E. D. Specht, D. Arena, F. J. Walker, and C. H. Ahn, APL Mater. **1**, 032110 (2013).
[37]S. Catalano, M. Gibert, V. Bisogni, O. E. Peil, F. He, R. Sutarto, M. Viret, P. Zubko, R. Scherwitzl, A. Georges, G. A. Sawatzky, T. Schmitt, and J.-M. Triscone, APL Mater. **2**, 116110 (2014).
[38]J. L. García-Muñoz, J. Rodríguez-Carvajal, P. Lacorre, and J. B. Torrance, Phys. Rev. B **46**, 4414 (1992).
[39]J. A. Alonso, M. J. Martínez-Lope, M. T. Casais, M. A. G. Aranda, and M. T. Fernández-Díaz, J. Am. Chem. Soc. **121**, 4754 (1999).
[40]J.-S. Zhou, J. Goodenough, and B. Dabrowski, Phys. Rev. B **67**, 020404 (2003).
[41]S. K. Ojha, S. Ray, T. Das, S. Middey, S. Sarkar, P. Mahadevan, Z. Wang, Y. Zhu, X. Liu, M. Kareev, and J. Chakhalian, Phys. Rev. B **99**, 235153 (2019).
[42]S. Middey, D. Meyers, R. Kumar Patel, X. Liu, M. Kareev, P. Shafer, J.-W. Kim, P. J. Ryan, and J. Chakhalian, Appl. Phys. Lett. **113**, 081602 (2018).
[43]J. L. García-Muñoz, J. Rodríguez-Carvajal, and P. Lacorre, Phys. Rev. B **50**, 978 (1994).
[44]V. Scagnoli, U. Staub, A. M. Mulders, M. Janousch, G. I. Meijer, G. Hammerl, J. M. Tonnerre, and N. Stojic, Phys. Rev. B **73**, 100409 (2006).
[45]S. Middey, D. Meyers, M. Kareev, Y. Cao, X. Liu, P. Shafer, J. W. Freeland, J.-W. Kim, P. J. Ryan, and J. Chakhalian, Phys. Rev. Lett. **120**, 156801 (2018).
[46]S. Middey, D. Meyers, M. Kareev, X. Liu, Y. Cao, J. W. Freeland, and J. Chakhalian, Phys. Rev. B **98**, 045115 (2018).
[47]S. Lafuerza, G. Subías, J. García, S. D. Matteo, J. Blasco, V. Cuartero, and C. R. Natoli, J. Phys.: Condens. Matter **23**, 325601 (2011).
[48]D. H. Douma, R. Ciprian, A. Lamperti, P. Lupo, E. Cianci, D. Sangalli, F. Casoli, L. Nasi, F. Albertini, P. Torelli, and A. Debernardi, Phys. Rev. B **90**, 205201 (2014).
[49]M. Medarde, A. Fontaine, J. L. García-Muñoz, J. Rodríguez-Carvajal, M. de Santis, M. Sacchi, G. Rossi, and P. Lacorre, Phys. Rev. B **46**, 14975 (1992).
[50]J. Liu, M. Kareev, B. Gray, J. W. Kim, P. Ryan, B. Dabrowski, J. W. Freeland, and J. Chakhalian, Appl. Phys. Lett. **96**, 233110 (2010).
[51]M. Wu, E. Benckiser, P. Audehm, E. Goering, P. Wochner, G. Christiani, G. Logvenov, H.-U. Habermeier, and B. Keimer, Phys. Rev. B **91**, 195130 (2015).
[52]S. Middey, P. Rivero, D. Meyers, M. Kareev, X. Liu, Y. Cao, J. W. Freeland, S. Barraza-Lopez, and J. Chakhalian, Sci. Rep. **4**, 6819 (2014).
[53]J. W. Freeland, M. van Veenendaal, and J. Chakhalian, "Special issue: Electronic structure and function from state-of-the-art spectroscopy and theory," J. Electron Spectrosc. Relat. Phenom. **208**, 56 (2016).
[54]D. Meyers, J. Liu, J. W. Freeland, S. Middey, M. Kareev, J. Kwon, J. M. Zuo, Y.-D. Chuang, J. W. Kim, P. J. Ryan *et al.*, Sci. Rep. **6**, 27934 (2016).
[55]K. Post, A. McLeod, M. Hepting, M. Bluschke, Y. Wang, G. Cristiani, G. Logvenov, A. Charnukha, G. Ni, P. Radhakrishnan *et al.*, Nat. Phys. **14**, 1056 (2018).
[56]M. H. Upton, Y. Choi, H. Park, J. Liu, D. Meyers, J. Chakhalian, S. Middey, J.-W. Kim, and P. J. Ryan, Phys. Rev. Lett. **115**, 036401 (2015).
[57]G. N. Daptary, S. Kumar, M. Kareev, J. Chakhalian, A. Bid, and S. Middey, Phys. Rev. B **100**, 125105 (2019).
[58]J. H. Park, J. M. Coy, T. S. Kasirga, C. Huang, Z. Fei, S. Hunter, and D. H. Cobden, Nature **500**, 431 (2013).